ACS OMEGA

Open Access

http://pubs.acs.org/journal/acsodf

Article

Microwave Synthesis of Carbon Quantum Dots from Arabica Coffee Ground for Fluorescence Detection of Fe^{3+}, Pb^{2+}, and Cr^{3+}

Muhammad Nazar, Muhammad Hasan,* Basuki Wirjosentono, Basri A. Gani, and Cut Elvira Nada

Cite This: *ACS Omega* 2024, 9, 20571−20581

Read Online

ACCESS | Metrics & More | Article Recommendations

ABSTRACT: In this study, carbon quantum dots (CQDs), which were synthesized from arabica coffee ground-derived activated carbon, have been successfully employed as a fluorescence sensor to detect Fe^{3+} ions. CQDs were fabricated using microwave heating for 5−10 min, which emitted vibrant blue light at 455 nm when exposed to excitation at 365 nm. Dynamic light scattering (DLS) analysis revealed that the average size of CQDs was 10.12 nm with a quantum yield of 6.01%. Fluorescence detection was developed for sensing Fe^{3+}, Pb^{2+}, and Cr^{3+} ions. The addition of the three metal ions resulted in a decrease in the fluorescence (FL) intensity of the CQDs, with the addition of Fe^{3+} ions demonstrating a more significant decrease in FL compared to the addition of both Cr^{3+} and Pb^{2+} ions. The results indicated that the CQDs synthesized from activated carbon of arabica coffee waste performed as a selective fluorescent detector for Fe^{3+} ions, with a detection limit of 0.27 μM.

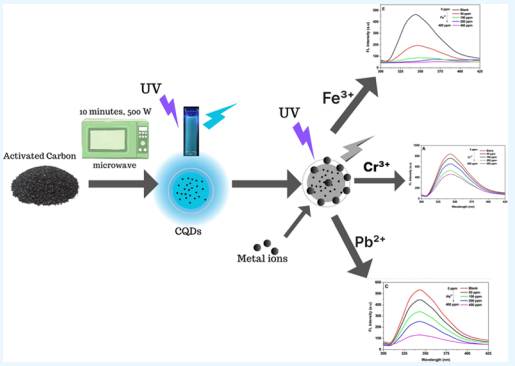

INTRODUCTION

Carbon quantum dots belong to the group of zero-dimensional nanostructure materials that have gained significant attention due to their unique properties such as the quantum energy level,[1] robust chemical inertness, excellent solubility in water, and strong luminescence properties.[2] CQDs have gradually become a prevalent material since their first fabrication in 2004 through electrophoresis[3] and later in 2006, which were prepared via laser ablation of graphite.[4] Currently, the production of CQDs using a wide range of raw materials has been extensively and intensively reported, including apple juice,[1] lemon juice,[5] tea,[6] fermented tea,[7] green tea,[8] lysine,[9] coffee grounds,[10] and lemon peel waste.[11]

CQDs are usually prepared by top-down and bottom-up methods.[12] In the top-down fabrication method, carbon mass is broken down into chemically treated or physically modified nanosized particles, such as ball-milling[13] or acid treatment. The resulting suspension is then filtered and washed to isolate the CQDs. The CQDs are usually stabilized using a capping agent, such as surfactants or polymers, to prevent aggregation. Finally, the stabilized CQDs are purified through centrifugation and redispersion to remove any remaining impurities.

On the other hand, the bottom-up method to synthesize carbon quantum dots involves using precursor materials such as carbon-rich organic compounds or graphene oxide, which are subjected to chemical or thermal treatment to generate the nanoscale dots. This process typically involves reducing the precursor materials to form the quantum dots and controlling the size and shape of the dots through variations in reaction conditions, such as temperature, reaction time, and the presence of stabilizing agents. The bottom-up method has the advantage of allowing for precise control over the dots' size and shape, which can significantly impact their optical and electronic properties. Additionally, this method can be easily scaled up for the large-scale production of carbon quantum dots.

Most of the synthesis processes usually involve various chemicals, which are complicated and involve multisteps. However, in this study, a simple microwave-assisted synthesis of CQDs from arabica coffee ground-derived activated carbon was successfully performed. The synthesis required only 10 min under microwave radiation without sample pretreatment, resulting in an economized and green synthesis of CQDs. The microwave technique is considered the most straightforward method that is frequently used to fabricate quantum dots.[9,14−22] The microwave method of synthesizing CQDs involves microwave radiation to irradiate a solution containing targeted precursors to produce nanoparticles. This method has become increasingly popular as it is a fast and efficient way to synthesize CQDs compared to other methods, such as chemical reduction and hydrothermal synthesis.[19,23] The microwave method can reduce synthesis times from several

Received: March 7, 2024
Revised: April 4, 2024
Accepted: April 11, 2024
Published: April 24, 2024

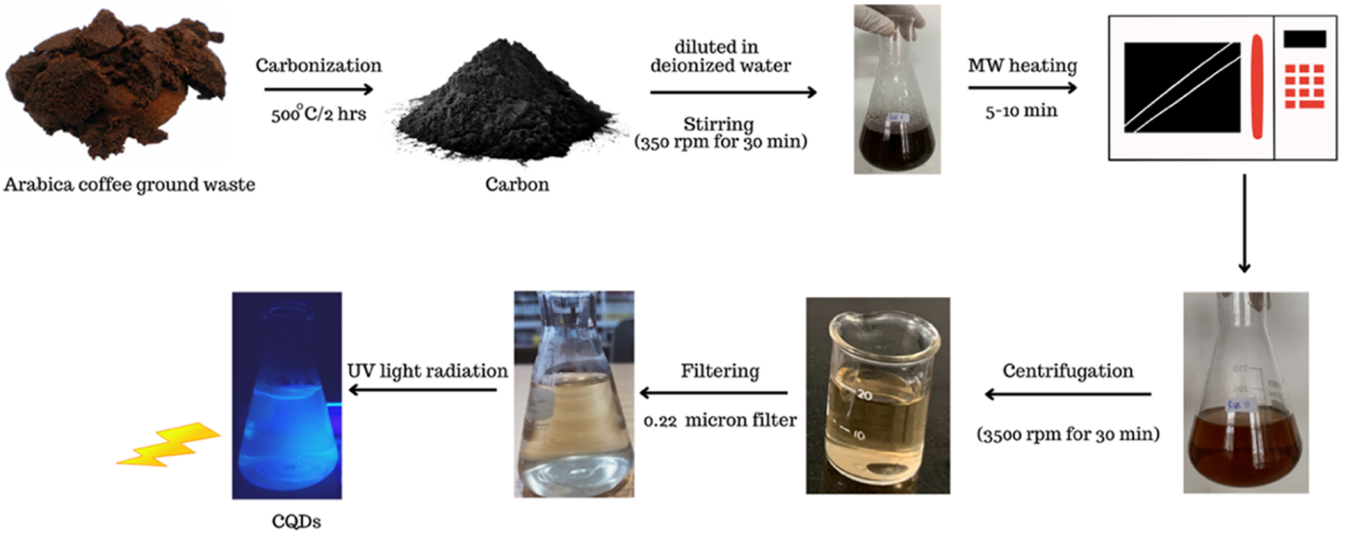

Figure 1. Schematic illustration for fabrication of CQDs via microwave heating.

hours to a few minutes, ensuring a more cost-effective and scalable approach in CQD synthesis. Additionally, the consistent heating process provided by microwave radiation leads to more homogeneous and well-controlled particle size and composition compared to other methods.[24,25] The properties of CQDs can also be tailored by controlling the synthesis conditions and the doping agent used, making them suitable for various applications, including bioimaging,[10,26−29] photovoltaics,[18,30,31] and sensing.[11,32]

Toxic heavy metal ions pose a significant threat to the environment, human health, and animal health.[33] Therefore, toxic metal ion detection techniques have seen much development. Current methods, including inductively coupled plasma mass spectrometry, atomic absorption spectrometry, atomic fluorescence spectrometry, potentiometry, and electrochemical techniques, are usually employed to detect heavy metal ions. Some of these approaches were nonportable, difficult, and somewhat costly. They also required time-consuming sample preparation processes.

Due to their simplicity, excellent sensitivity and selectivity, quick reaction times, little interference effects, and relative affordability, fluorescence-based sensors such as CQDs have recently gained more and more attention.[34] The fluorescent CQDs in an aqueous solution could be quenched by an electron acceptor or an electron donor, and the photoinduced electron-transfer properties of CQDs can be utilized to detect metal ions using nanoscale probes.[35] Therefore, rapid qualitative and quantitative detection of heavy metal ions in an aqueous solution is of great research value.[36] Several studies have proven that CQDs can be used as metal ion detectors, such as Fe^{2+} and Fe^{3+},[37−39] Cu^{2+},[34] Pb^{2+},[40] and Cr^{6+}.[41,42] In this work, we proposed fluorescent detection of Fe^{3+}, Cr^{3+}, and Pb^{2+} ions using CQDs generated from the arabica coffee-derived AC.

MATERIALS AND METHODS

Chemicals. Arabica coffee ground (ACG) was obtained from a local coffee shop in Banda Aceh, Indonesia. Ultrapure water was purchased from Merck, Germany. All chemicals, including $Pb(NO_3)_2$, $FeCl_3$, Cr_2O_3, $ZnCl_2$, HCl, and NaOH for carbon black activation, were purchased from Sigma-Aldrich, Singapore, and were used without further purification.

Instrumentation. The synthesis was performed using a microwave (Rewez P4020DL-K8, Japan). The resulting CQDs were dried using an oven (Memmert, Germany). An ultraviolet−visible (UV−vis) spectrophotometer, Shimadzu, UV1800, Japan, was used to analyze the absorption spectra of the CQDs. Photoluminescence spectra of the CQDs were measured using a spectrofluorophotometer model RF-5301PC, Shimadzu, Japan. CQDs' particle size distribution was determined by a transmission electron microscope (TEM, JEOL JEM-1400, Japan). Functional groups of both AC and CQDs were analyzed using an FTIR-8400s, Shimadzu, Japan. The particle size of the CQDs was analyzed using a dynamic light scattering instrument (Zetasizer Lab, Malvern)

Synthesis of CQDs. CQDs' synthesis was performed according to previous works[16,43] with slight modification. A desired mass of AC was carefully weighed using an analytical electronic balance (Ohaus CV314C) and transferred to a beaker glass. Two hundred milliliters of ultrapure water was added, and the AC suspension was stirred at 1500 rpm for 30 min using a magnetic stirrer (JoanLab SH-2, China) and transferred to a conical flask. It was then irradiated under microwave power for 3−7 min. The resulting pale brown mixture was centrifuged at 3500 rpm for 30 min to remove impurities; the supernatant was then filtered using filter paper (Whatman, No. 40) and further purified using a 0.22 μm nylon filter syringe. The pure CQDs were then dried using an oven until solid brownish CQDs were obtained.

Figure 1 depicts the schematic synthesis of CQDs by using the microwave method. As reported earlier, the carbon used in this work was physicochemically activated using $ZnCl_2$ combined with microwave radiation.[44] The AC was directly used to synthesize the CQDs without further treatment. The resulting CQDs were also found thermally stable since they were not degraded or damaged after being completely dried using the oven at 120 °C for 10 h (Figure 2).

Relative Quantum Yield Determination. The quantum yield (QY) of the CQDs was calculated by comparing the integrated luminescence intensities and absorbance values of the sample by following the standardized procedure.[45] Concisely, the desired amount of CQDs was carefully weighed using an analytical balance and diluted in pure water (η = 1.33), the reference chemical (quinine sulfate) was dissolved in

https://doi.org/10.1021/acsomega.4c02254
ACS Omega 2024, 9, 20571−20581

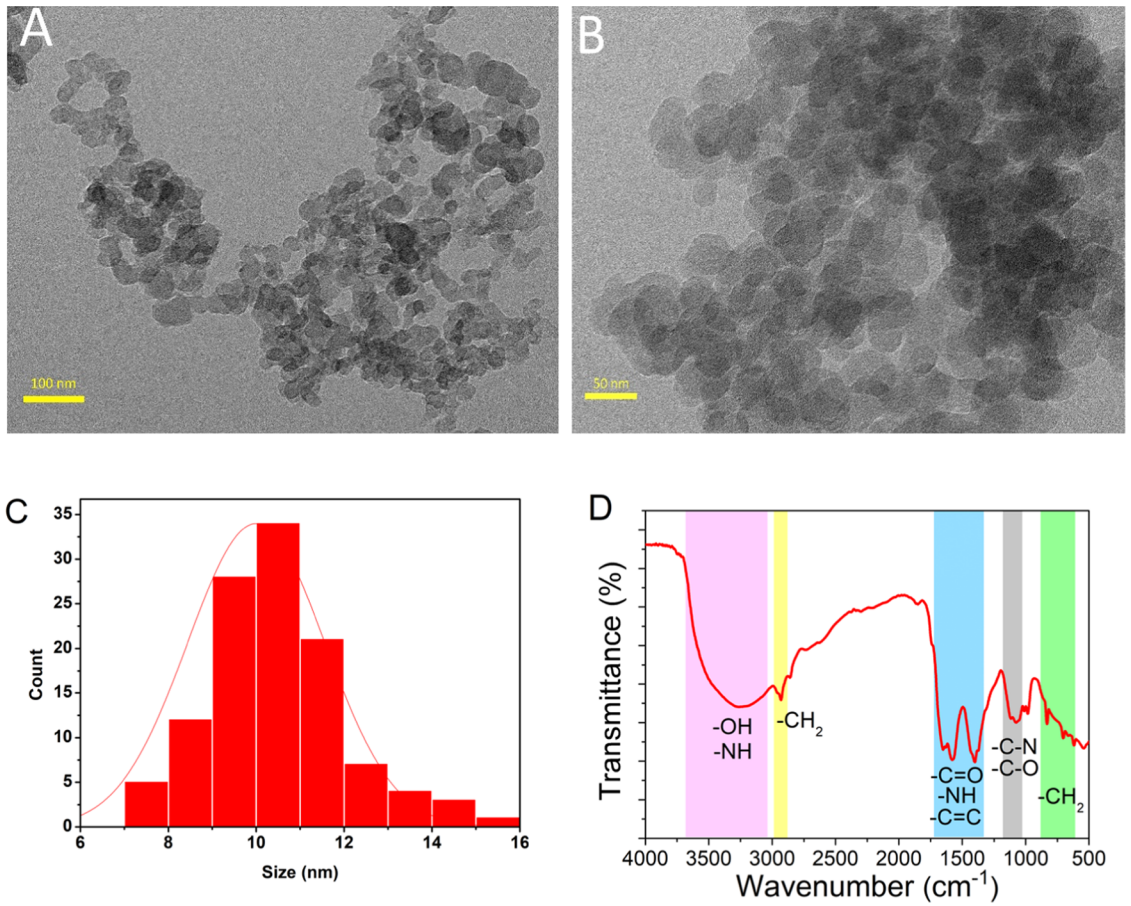

Figure 2. HRTEM image of CQDs (A) 100 nm and (B) 50 nm. (C) Particle size distribution of CQDs measured by DLS and (D) FTIR spectra.

a sulfuric acid solution (H_2SO_4, 0.1 M), and the absorbance of both the sample and the reference were recorded at 350 nm. The sample QY was calculated using the following equation:

$$\Phi = \Phi_R \times \frac{I}{I_R} \times \frac{A_R}{A} \times \frac{\eta^2}{\eta_R^2} A$$

where Φ, I, A, and η are QY, FL intensity, absorbance, and refractive index, respectively, Φ_R is QY of the quinine sulfate = 54%,[46] and R stands for reference.

Detection of Fe^{3+}, Pb^{2+}, and Cr^{3+} Ions. To examine the sensing ability of CQDs against the metal ions, a 1000 ppm stock solution of CQDs was prepared by adding it to a desired volume of ultrapure water. The metal ions Pb^{2+}, Cr^{3+}, and Fe^{3+} at various concentrations (50−400 ppm) were prepared separately. In order to evaluate the sensitivity of metal ions, each metal ion with varied concentrations was added to the CQDs solution, and the FL spectra were recorded at the maximum excitation wavelength, 224 nm. FL spectra were then used to compare their quenching efficiency.

RESULTS AND DISCUSSION

The conversion of CQDs from arabica coffee ground-derived AC utilizing microwave irradiation has been successfully conducted. The optimum conditions for the CQD fabrication was achieved at the contact time of 8 min, 1.5 g of starting material, and 80% power of a 800 W microwave oven, as previously reported.[43] The pale brown solution of CQDs observed under daylight was characterized using HRTEM, FTIR spectrophotometer, DLS, and a fluorescence spectrophotometer.

The microscopic properties of the CQDs were determined using HRTEM analysis, indicating that the particles were spherical, homogeneously monodispersed, and with no form of aggregation. The CQDs' particle distribution confirms the small particle size ranging from 7 to 16 nm (mean = 10.12 nm, SD ± 1.76). The CQDs fabricated in this study met the criteria of nanosized material when compared to some previous studies, as depicted in Table 1.

The FTIR spectra of CQDs confirm the presence of OH groups (3246 cm^{-1}) and C═C stretching (1650 cm^{-1}), while the FTIR spectra of the AC used as a precursor for preparing CQDs do not exhibit a OH spectrum but show weak N−H stretching at 3633 cm^{-1}. The FTIR spectrum of the precursor also indicates the presence of C═O and C═C (1650 and 1577 cm^{-1}) at much lower intensity (Figure 3). The vigorous intensity of the absorption of OH, CH, C═O, C−O, and conjugated C═C in CQDs is attributed to their small particle size, which ranges from 1 to 10 nm and is linked to their larger surface area, which is associated with a more significant number of functional groups appearing on the surface of CQDs.[55] The above investigations suggested that CQDs were functionalized with hydroxyl, carboxylic, carbonyl, and amino groups, derived from organic moiety-activated carbon with microwave synthesis.

The photoluminescence characteristics of CQDs may be affected by diverse functional groups present on their surfaces, such as carboxyl (−COOH), amino ($-NH_2$), hydroxyl

https://doi.org/10.1021/acsomega.4c02254
ACS Omega 2024, 9, 20571−20581

Table 1. Particle Size of CQDs Produced from Different Precursors

no	precursor	method	particle size range (nm)	reference
1	cranberry beans	hydrothermal	1.23−6.63	47
2	table sugar	microwave	2.50−5.50	48
3	lemon juice	hydrothermal	30−80	5
4	starch	microwave	2−4	14
5	*Calotropis gigantea*	microwave	2.7−10.4	17
6	eggshell	microwave	0.56−3.88	49
7	sucrose	hydrothermal	4−15	50
8	coconut shell	hydrothermal	3−5	51
9	broccoli	hydrothermal	2−6	52
10	aloe vera	facile carbonization	4−10	53
11	kelp	microwave	3−4.4	20
12	apple juice	hydrothermal	5−10	1
13	sugar cane	hydrothermal	2−8	54
14	Arabica coffee ground	microwave	7−16	this work

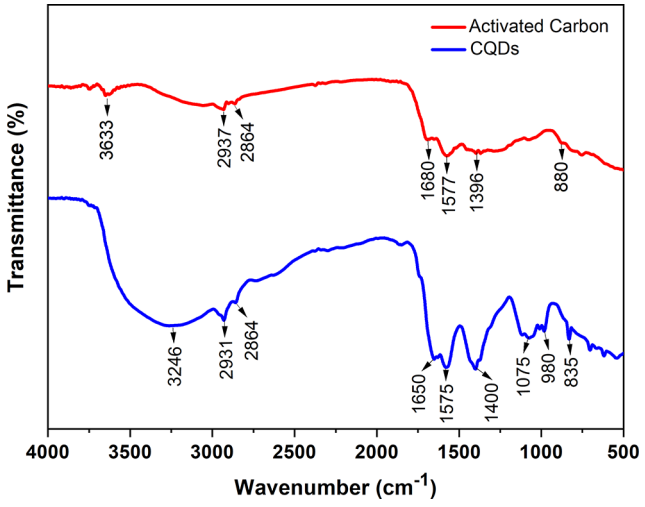

Figure 3. FTIR spectra of CQDs and their precursor of Arabica coffee ground activated carbon.

(−OH), and carbonyl (C═O) groups. These groups can alter CQDs' surface states, passivation, and trap states, thereby influencing their photoluminescence properties, such as quantum yield, emission wavelength, and lifetime. Typically, a CQD would absorb the UV light and emit visible rays. When CQDs are irradiated with UV light, the energy from the photons is absorbed by the electrons, which elevate them to a higher energy state (excited state). However, due to their small size and high surface-to-volume ratio, CQDs exhibit quantum confinement effects that result in discrete energy levels rather than the continuous energy bands observed in bulk semiconductors.

Therefore, the high-energy states created in CQDs are highly localized, and the electrons rapidly transition back to their underlying ground state. In this process, excess energy is released as a photon, and the wavelength of this photon corresponds to the energy difference between the excited and the ground states. For CQDs, this energy difference falls within the visible-light range, resulting in visible-light emission. The emission was confirmed by fluorescence spectroscopy analysis of the CQDs, as depicted in Figure 4. Typical CQDs emit visible light ranging from 350 to 650 nm, depending on the precursors used for synthesis.

The CQDs emit pale blue visible light at the wavelength of around 280 to 600 nm, with the most intensive emission at 455 nm.[56] The CQDs produced in this work have shown the capacity to absorb UV at a maximum wavelength of 224 nm, which corresponds to electron promotion from $\pi \rightarrow \pi^*$; this transition typically occurs in unsaturated hydrocarbon molecules or molecules with double bonds, which is also confirmed by FTIR spectra (Figure 3). The energy band gap of the CQDs was also determined using Tauc's plot. The absorbance spectrum of CQDs shows an optical energy gap of 6.06 eV (Figure 4C); this value is relatively higher compared to previously synthesized CQDs. Sutanto et al.[57] reported successful synthesis of CQDs from citric acid and urea with an energy gap ranging from 1.5 to 2.5 eV. Another study by Bao et al.[3030] revealed that the energy gap of a carbon dot is dictated by the particle size of the CQDs; the smaller the particle, the greater the energy gap between the valence and the conduction band due to the conjugate effect or the quantum-size effect.

Following their dissolution in water, AC and CQDs vary significantly in visible light. A CQD solution has a light brown color and emits blue light when exposed to UV light, while AC is difficult to dissolve in water and forms a clear solution and shows a very weak ability to emit visible light when exposed to UV light. FL Intensity measurement (Figure 5B) shows that the aqueous solution of CQDs is highly fluorescent.

Figure 6 shows the results of the 15 h CQD stability test. Water-dispersed CQDs were exposed to direct sunlight for 15 h and observed under UV light every 5 h. Visually, the color of the CQD solution under visible light did not show any significant degradation. However, when observed under UV light, the fluorescence properties of the CQDs decreased with increasing time. In addition, Figure 5B confirms the gradual decrease in the ability of CQDs to emit visible light after being exposed to direct sunlight for a period of time. CQDs' exposure to sunlight for a duration of 15 h results in a reduction exceeding 70% in the visible-light-emission capacity of CQDs (Figure 6).

The diminishing capacity of CQDs to absorb UV and emit visible light is associated with the reduction of functional groups responsible for these processes, such as OH, C═O, and N−H groups. Fluorescent materials usually fade over time when exposed to light, emphasizing the need for high photostability in applications requiring prolonged light exposure. Previous studies revealed that the stability of CQDs is significantly affected by several factors such as UV and visible-light radiation,[58] temperature,[59] pH,[60] and salt solutions including NaCl or KCl.[61] Therefore, the photostability of CQDs should be evaluated by considering these parameters.[62]

Quantum Yield (QY). The QY pertains to the ratio of fluorescence intensity emitted by nanomaterials concerning absorbed excitation. As the fluorescence intensity increases, the QY of the CQDs also increases. The fluorescence mechanism of nanoparticles relies on two principal factors: surface state defects or alterations in surface conditions and quantum confinement.[31,35] Surface state defects or changes in surface conditions cause modifications in the optical properties of nanoparticles, including fluorescence intensity, excitation wavelength, and radiation. These effects stem from the fact that nanoparticles predominantly consist of a limited number

https://doi.org/10.1021/acsomega.4c02254
ACS Omega 2024, 9, 20571−20581

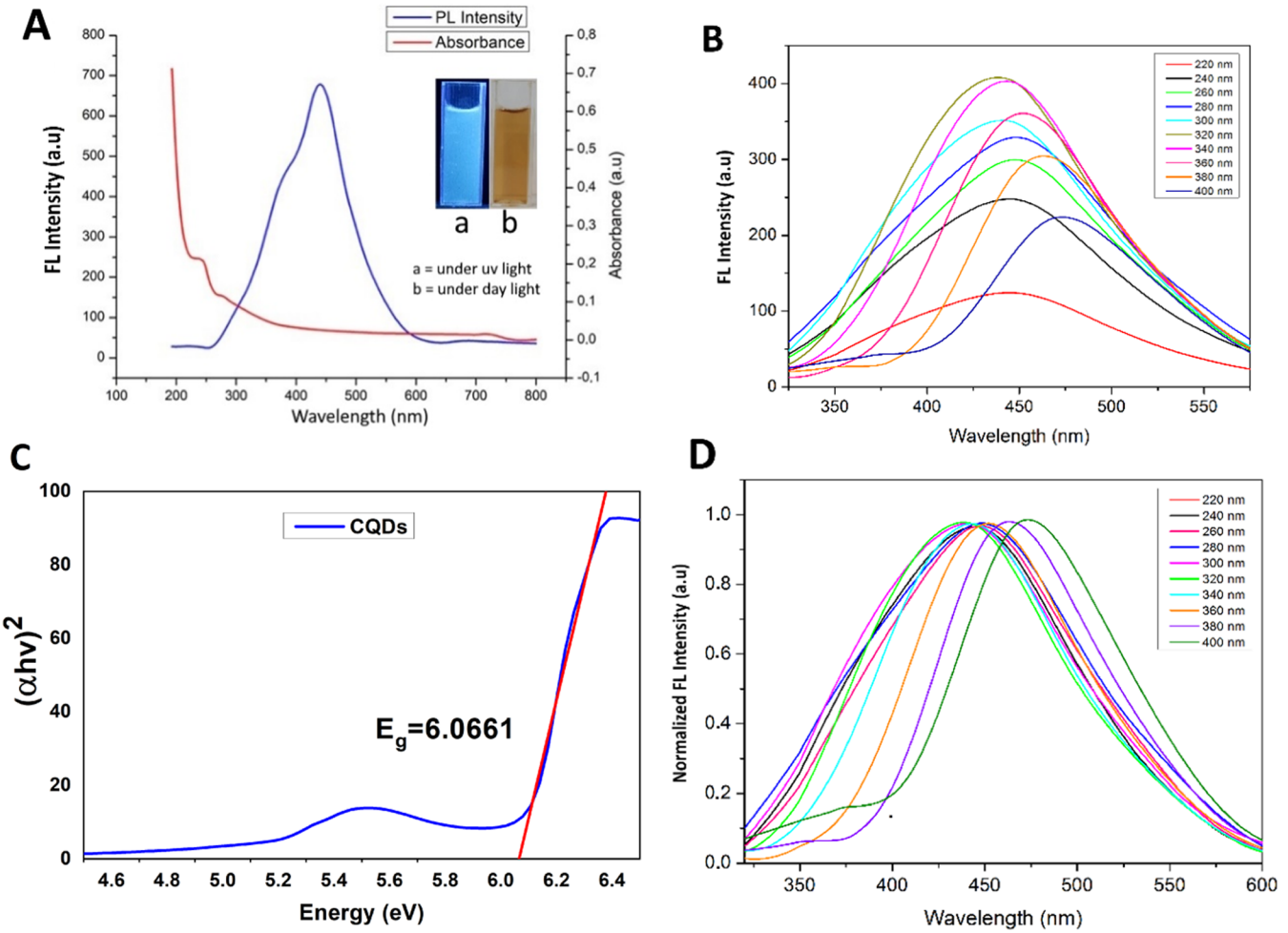

Figure 4. (A) UV−vis spectrum (abs) compared to FL intensity of the CQDs at an excitation wavelength of 224 nm. (B) FL intensity of the CQDs measured at different excitation wavelengths. (C) Direct band gap determined using the Tauc plot. (D) Normalized FL intensity of CQDs at various excitation wavelengths (220−400 nm).

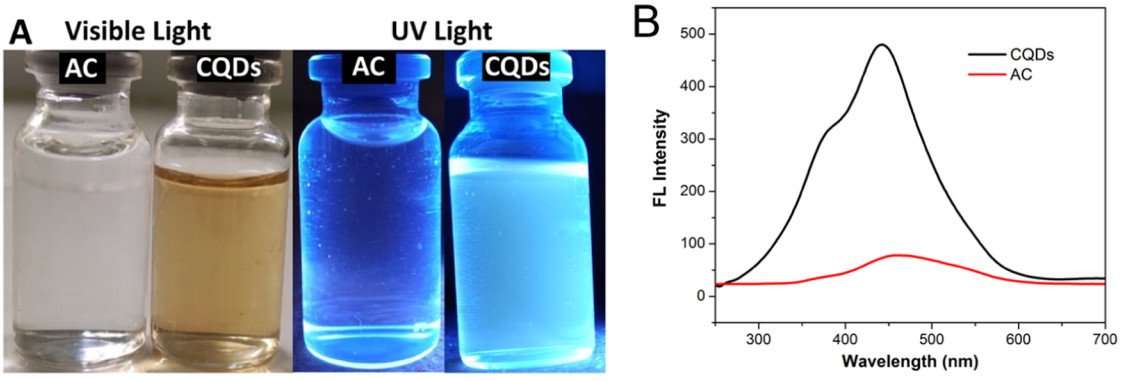

Figure 5. (A) Water-dispersed AC and CQDs observed under visible light and UV light. (B) FL intensity of the aqueous solution of AC and CQDs.

of atoms, mainly situated on their surfaces, thereby rendering any surface changes influential on the nanoparticle properties. Quantum confinement theory elucidates that all particles are constrained within the band gap formed by the highest occupied molecular orbital (HOMO) and the lowest unoccupied molecular orbital (LUMO).[63] Diminishing particle size enhances the energy gap between these orbitals, resulting in greater energy demand for electrons in the HOMO orbital to be excited to the LUMO orbital. Consequently, electrons relax and return to the ground by emitting light upon excitation. The magnitude of the energy gap, thus, determines the emission wavelength of nanoparticles.[64]

The CQDs produced in this study have a QY value of 6% relative to that of quinine sulfate (54%). This QY value is in good agreement with previous studies that produced CQDs with yields up to 5%, even though some studies have reported higher QY values, such as refs 2,4,31,65−67. These studies reported a higher QY that was achieved by doping the starting

https://doi.org/10.1021/acsomega.4c02254
ACS Omega 2024, 9, 20571−20581

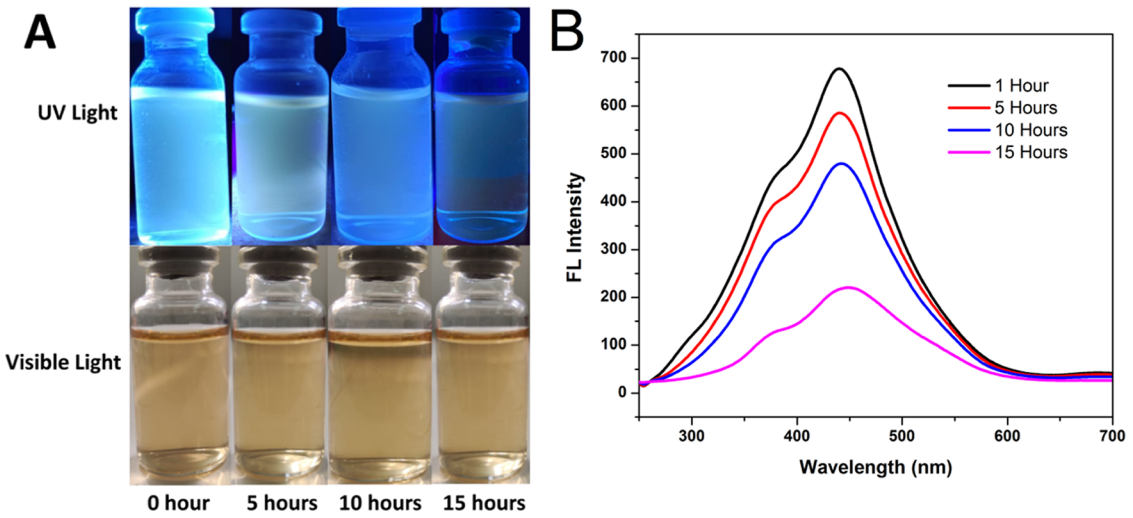

Figure 6. Stability of the CQDs when exposed to sunlight at ambient temperature from 1 to 15 h (A) observed under UV light and visible light. (B) FL intensity of CQDs after being exposed to the sunlight for up to 15 hours.

materials with nitrogen-rich compounds for more functional groups corresponding to higher light-emission rates.

Table 2 shows the QY values of CQDs synthesized using different precursors. Both pure chemicals and plant material extracts can produce CQDs with higher QY. On the other hand, waste precursors, especially coffee waste, yielded lower QY due to the minimum content of carbon−nitrogen compounds remaining in coffee grounds. Despite attempts at carbonation, as performed in our research, a significant increase in the QY values has yet to be achieved. Carbonation and activation of carbon obtained from arabica coffee grounds contribute to a 20% increase in QY compared to the previous study.[71]

Table 2. Quantum Yield of CQDs Derived from Different Precursors

precursor	quantum yield (%)	reference
arginine	17.0	68
lemon juice	24.9	69
used coffee ground	3.8	70
coffee ground	5.0	71
Arabica coffee ground AC	6.0	this work

Heavy Metal Detection. Some previous studies have revealed the potential of CQDs as sensors for metals such as Fe^{3+} and Cu^{2+}. However, they have shown limited efficacy in detecting other metals due to their low sensitivity and high limit of detection (LOD). The ions such as Cu^{2+}, K^{+}, Ca^{2+}, Pb^{2+}, Hg^{2+}, Fe^{2+}, and Fe^{3+} are frequently being studied for their interactions with CQDs. In this study, the focus shifted to three metal ions, Cr^{3+}, Pb^{2+}, and Fe^{3+}, because these three metal ions are frequently used in the chemistry lab. The test results indicate that the FL intensity of the CQDs decreases gradually when interacting with the targeted metal ions at various concentrations but possesses different magnitudes and patterns. Optical studies of desired metal ion quenching using a UV−vis spectrophotometer show significantly different patterns of absorbance due to the addition of the metal ions at different concentrations, particularly Fe^{3+}, which exhibits shifted shoulder peaks.

When Cr^{3+}, Pb^{2+}, and Fe^{3+} ions with similar concentrations were added to the CQD solution at ambient temperature, FL intensity degradation was observed (Figure 7). However, the results indicate that the FL intensity of CQDs decreases when interacting with Fe^{3+} is more noticeable compared to Cr^{3+} or Pb^{2+} ions (Figure 7E). Specifically, the addition of 50 ppm Fe^{3+} ions shows a significant and sharp decrease in FL intensity, dropping from 462 (blank) to 196, representing a reduction of over 50% in the FL intensity of CQDs. In contrast, adding 50 ppm Cr^{3+} and Pb^{2+} ions has only resulted in 16 and 9% reductions in the FL intensity of CQDs, respectively. Moreover, the interaction between Fe^{3+} ions and CQDs induces a noticeable shift in the emission peak from 343 to 370 nm, as depicted in Figure 4E. However, this shift in the emission peak is not observed in the FL spectra of both Cr^{3+} and Pb^{2+}. The optical studies also reveal that the lowest concentration of Fe^{3+} was able to decrease the FL intensity of CQDs much more significantly compared to Cr^{3+} and Pb^{2+}.

The linear relationship between the relative FL intensity values and the addition of each metal ion at different concentrations was also investigated (Figure 8). Based on the linear correlation between the relative FL intensity of the metal ion samples and their respective concentrations, it is evident that all three metals, Cr^{3+}, Pb^{2+}, and Fe^{3+}, exhibit linear solid correlations with *R*-squared (R^2) values of 0.985, 0.998, and 0.995, respectively. However, when comparing the values of relative FL intensities (F_0/F) after the addition of 400 ppm Cr^{3+}, Pb^{2+}, and Fe^{3+}, the values of relative FL intensities of both ions were found to be 1.9, 4.0, and 9.8, respectively (Figure 7A,C), and the (F_0/F) values of Fe^{3+} ions were twice greater than Pb^{2+} ions and about four times greater when compared to the Cr^{3+} ions. The differences in the relative FL intensity indicate that CQDs interacted more effectively with Fe^{3+} ions compared to Cr^{3+} and Pb^{2+}.

The addition of Fe^{3+} ions results in a decrease in emission intensity at 344 nm. This decrease is attributed to carboxyl (−COOH) groups, which undergo deprotonation to generate carboxylate ions (−COO). This deprotonation process facilitates the formation of complex ions with Fe^{3+}, contributing to the detection mechanism.[72] This finding further confirms the selectivity of CQDs toward Fe^{3+} ions, thereby suggesting that CQDs derived from arabica coffee

https://doi.org/10.1021/acsomega.4c02254
ACS Omega 2024, 9, 20571−20581

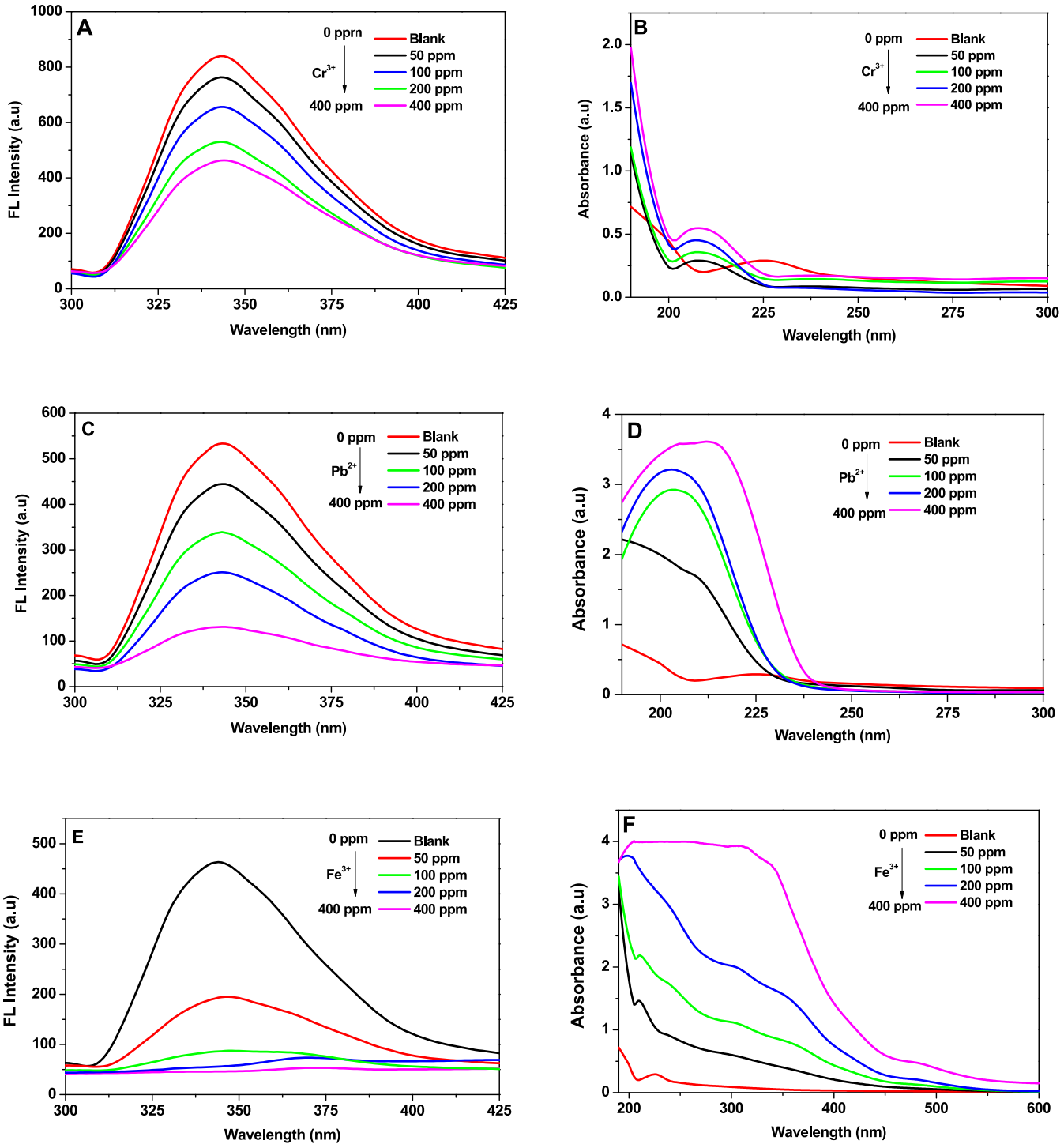

Figure 7. (A, B) FL intensity and absorbance of quenching CQDs on the addition of varied concentrations of Cr^{3+}. (C, D) FL intensity and absorbance of quenching CQDs on the addition of varied concentrations of Pb^{2+}. (E, F) FL intensity and absorbance of quenching CQDs on the addition of varied concentrations of Fe^{3+}.

waste-activated carbon can be utilized as a selective fluorescence sensor for Fe^{3+}-ion detection with a detection limit of 0.27 μM. The study on the utilization of CQDs as a fluorescent detector of Fe^{3+} ions has garnered considerable attention. Vadia et al. synthesized CQDs from a lemon peel with an impressive quantum yield (QY) of 32% and capable of detecting Fe^{3+} ions at a better detection limit of 0.18 μM.[73] Other studies conducted by Khan et al.[74] and Wang et al.[75] have also reported successful deployment of CQDs as fluorescent sensors for detecting the Fe^{3+} ion.

CONCLUSIONS

In this study, the synthesis of CQDs from arabica coffee grounds using a simple and cost-effective method of microwave irradiation has been successfully performed. The characteristics of CQDs, including particle size, photoluminescent properties, FTIR analysis, optical evaluation, and fluorescence light

https://doi.org/10.1021/acsomega.4c02254
ACS Omega 2024, 9, 20571−20581

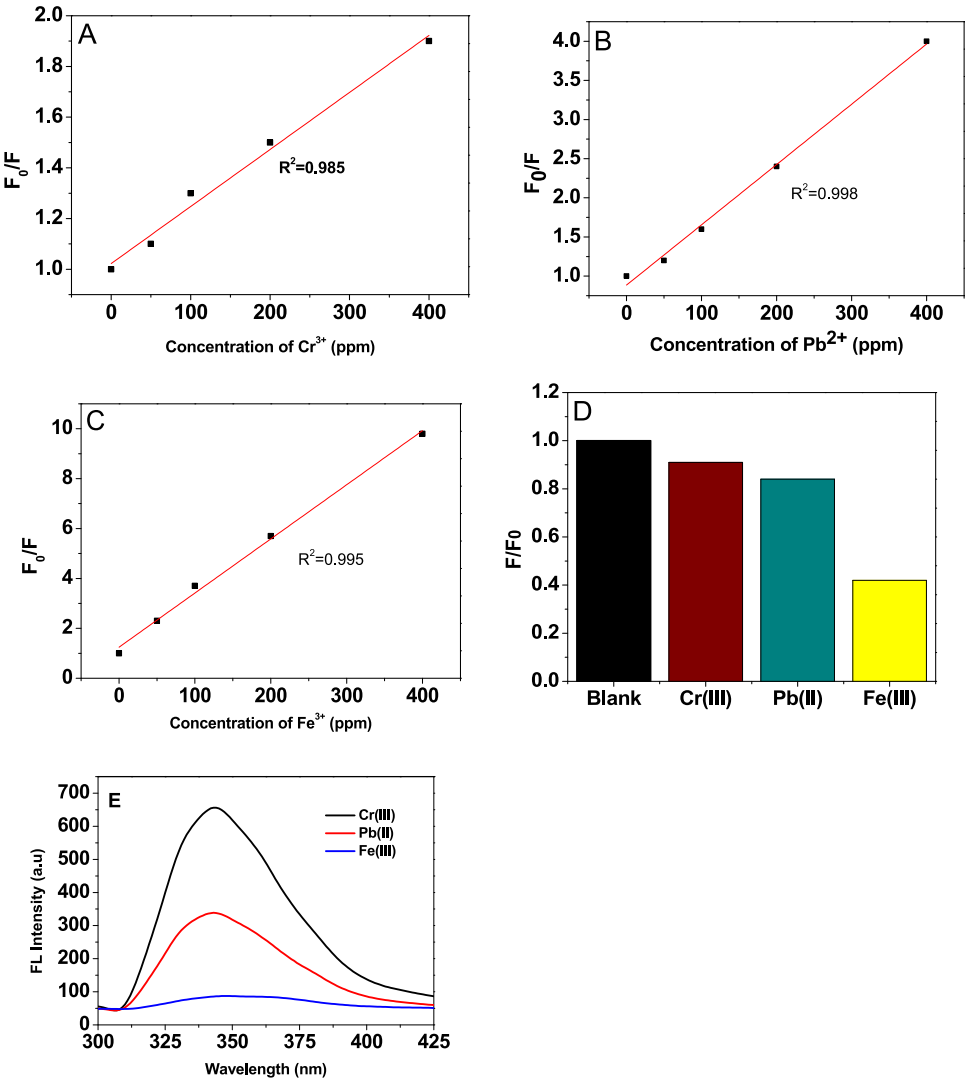

Figure 8. (A–C) Linear relationship of relative FL intensity of quenching CQDs and the concentrations of Cr^{3+}, Pb^{2+}, and Fe^{3+} ions, respectively, ranging from 50 to 400 ppm. (D) Relative FL intensities (F/F_0) of a blank CQD compared to the addition of metal ions (λ_{ex} = 224 nm, metal ions concentrations = 400 ppm). (E) FL intensities of CQDs on addition of metal ions (100 ppm, λ_{ex} = 224 nm).

emitting properties, were investigated using a proper apparatus. The quantum-sized particles fabricated in this study can absorb the energy in the ultraviolet wavelength and emit a glowing vibrant blue light at the wavelength ranging from 330 to 600 nm when excited at different wavelengths (220–400 nm). Further evaluation of the CQDs' interaction with three different metal ions, including Cr^{3+}, Pb^{2+}, and Fe^{3+}, revealed that the CQDs are highly selective to Fe^{3+} ions and thus can be utilized as a fluorescent detector of the ferric ions.

AUTHOR INFORMATION

Corresponding Author

Muhammad Hasan − *Department of Chemistry Education, Universitas Syiah Kuala, Banda Aceh 23111, Indonesia*; Email: muhammadhasan.kimia@usk.ac.id

Authors

Muhammad Nazar − *Graduate School of Mathematics and Applied Sciences, Universitas Syiah Kuala, Banda Aceh 23111, Indonesia; Department of Chemistry Education, Universitas Syiah Kuala, Banda Aceh 23111, Indonesia*; orcid.org/0000-0001-8361-606X

Basuki Wirjosentono − *Department of Chemistry, Universitas Sumatera Utara, Medan 20155, Indonesia*

Basri A. Gani − *Department of Oral Biology, Dentistry Faculty, Universitas Syiah Kuala, Banda Aceh 23111, Indonesia*

Cut Elvira Nada − *Department of Chemistry Education, Universitas Syiah Kuala, Banda Aceh 23111, Indonesia*

Complete contact information is available at: https://pubs.acs.org/10.1021/acsomega.4c02254

Author Contributions

M.N.: contributed to conceptualization, conducting the experiments, methodology, and preparing the original draft and all figures and tables. M.H.: contributed to the validation, result validation, and editing of the manuscript. B.W.: contributed to the investigation, review, and editing of the manuscript. B.A.G.: contributed to the conceptualization, supervision, and editing of the manuscript. C.E.N.: contributed to analyzing data and language editing. All authors have read and agreed to the final version of the manuscript.

https://doi.org/10.1021/acsomega.4c02254
ACS Omega 2024, 9, 20571−20581

Notes

The authors declare no competing financial interest.

■ ACKNOWLEDGMENTS

The authors acknowledge the Research Center for Nanoscience and Nanotechnology (RCNN) for HRTEM analysis and the Laboratory of Biochemistry, Faculty of Natural Sciences, Institut Teknologi Bandung, for fluorescence analysis.

■ REFERENCES

(1) Borna, S.; Sabzi, R. E.; Pirsa, S. Synthesis of Carbon Quantum Dots from Apple Juice and Graphite: Investigation of Fluorescence and Structural Properties and Use as an Electrochemical Sensor for Measuring Letrozole. *J. Mater. Sci.: Mater. Electron.* **2021**, *32* (8), 10866−10879.

(2) Wang, Y.; Hu, A. Carbon Quantum Dots: Synthesis, Properties and Applications. *J. Mater. Chem. C Mater.* **2014**, *2* (34), 6921−6939.

(3) Xu, X.; Ray, R.; Gu, Y.; J Ploehn, H.; Gearheart, L.; Raker, K.; A Scrivens, W. Electrophoretic Analysis and Purification of Fluorescent Single-Walled Carbon Nanotube Fragments. *J. Am. Chem. Soc.* **2004**, *126* (40), 12736−12737.

(4) Sun, Y. P.; Zhou, B.; Lin, Y.; Wang, W.; Fernando, K. A. S.; Pathak, P.; Meziani, M. J.; Harruff, B. A.; Wang, X.; Wang, H.; Luo, P. G.; Yang, H.; Kose, M. E.; Chen, B.; Veca, L. M.; Xie, S. Y. Quantum-Sized Carbon Dots for Bright and Colorful Photoluminescence. *J. Am. Chem. Soc.* **2006**, *128* (24), 7756−7757.

(5) Hoan, B. T.; Tam, P. D.; Pham, V. H. Green Synthesis of Highly Luminescent Carbon Quantum Dots from Lemon Juice. *J. Nanotechnol.* **2019**, *2019*, No. 2852816, DOI: 10.1155/2019/2852816.

(6) Zhu, J.; Zhu, F.; Yue, X.; Chen, P.; Sun, Y.; Zhang, L.; Mu, D.; Ke, F. Waste Utilization of Synthetic Carbon Quantum Dots Based on Tea and Peanut Shell. *J. Nanomater.* **2019**, *2019*, No. 7965756, DOI: 10.1155/2019/7965756.

(7) Baslak, C.; Demirel, S.; Kocyigit, A.; Alatli, H.; Yildirim, M. Supercapacitor Behaviors of Carbon Quantum Dots by Green Synthesis Method from Tea Fermented with Kombucha. *Mater. Sci. Semicond. Process* **2022**, *147* (November2021), No. 106738.

(8) He, Z.; Cheng, J.; Yan, W.; Long, W.; Ouyang, H.; Hu, X.; Liu, M.; Zhou, N.; Zhang, X.; Wei, Y. One-Step Preparation of Green Tea Ash Derived and Polymer Functionalized Carbon Quantum Dots via the Thiol-Ene Click Chemistry. *Inorg. Chem. Commun.* **2021**, *130* (June), No. 108743.

(9) Park, S. Y.; Thongsai, N.; Chae, A.; Jo, S.; Kang, E. B.; Paoprasert, P.; Park, S. Y.; In, I. Microwave-Assisted Synthesis of Luminescent and Biocompatible Lysine-Based Carbon Quantum Dots. *J. Ind. Eng. Chem.* **2017**, *47*, 329−335.

(10) Wang, L.; Li, W.; Wu, B.; Li, Z.; Wang, S.; Liu, Y.; Pan, D.; Wu, M. Facile Synthesis of Fluorescent Graphene Quantum Dots from Coffee Grounds for Bioimaging and Sensing. *Chem. Eng. J.* **2016**, *300*, 75−82.

(11) Tyagi, A.; Tripathi, K. M.; Singh, N.; Choudhary, S.; Kumar Gupta, R. Green Synthesis of Carbon Quantum Dots from Lemon Peel Waste: Applications in Sensing and Photocatalysis. *RSC Adv.* **2016**, *6*, 72423−72432, DOI: 10.1039/c6ra10488f.

(12) Sagbas, S.; Sahiner, N.Carbon Dots: Preparation, Properties, and Application. In *Nanocarbon and Its Composites: Preparation, Properties and Applications*; Elsevier, 2019; pp 651−676 DOI: 10.1016/B978-0-08-102509-3.00022-5.

(13) Zhou, J.; Dong, Y.; Ma, Y.; Zhang, T. Ball-Milling Graphite Used for Synthesis of Biocompatible Blue Luminescent Graphene Quantum Dots. *Adv. Res. Text Eng.* **2021**, *6* (2), No. 1064, DOI: 10.26420/advrestexteng.2021.1064.

(14) Shibata, H.; Abe, M.; Sato, K.; Uwai, K.; Tokuraku, K.; Iimori, T. Microwave-Assisted Synthesis and Formation Mechanism of Fluorescent Carbon Dots from Starch. *Carbohydr. Polym. Technol. Appl.* **2022**, *3*, No. 100218, DOI: 10.1016/j.carpta.2022.100218.

(15) Liu, Q. S.; Zheng, T.; Wang, P.; Guo, L. Preparation and Characterization of Activated Carbon from Bamboo by Microwave-Induced Phosphoric Acid Activation. *Ind. Crops Prod.* **2010**, *31* (2), 233−238.

(16) Chae, A.; Choi, Y.; Jo, S.; Nur'aeni; Paoprasert, P.; Park, S. Y.; In, I. Microwave-Assisted Synthesis of Fluorescent Carbon Quantum Dots from an A2/B3Monomer Set. *RSC Adv.* **2017**, *7* (21), 12663−12669.

(17) Sharma, N.; Sharma, I.; Bera, M. K. Microwave-Assisted Green Synthesis of Carbon Quantum Dots Derived from Calotropis Gigantea as a Fluorescent Probe for Bioimaging. *J. Fluoresc.* **2022**, *32* (3), 1039−1049.

(18) Jiang, X.; Luo, Z.; Zhang, B.; Li, P.; Xiao, J.; Su, W. Moderate Microwave-Assisted Preparation of Phthalocyanine-Based Carbon Quantum Dots for Improved Photo-Inactivation of Bacteria. *Inorg. Chem. Commun.* **2022**, *142* (May), No. 109543.

(19) Liu, P.; Wu, Z.; Ge, X.; Yang, X. Hydrothermal Synthesis and Microwave-Assisted Activation of Starch-Derived Carbons as an Effective Adsorbent for Naphthalene Removal. *R. Soc. Chem. Adv.* **2019**, *9* (21), 11696−11706.

(20) Zhao, C.; Li, X.; Cheng, C.; Yang, Y. Green and Microwave-Assisted Synthesis of Carbon Dots and Application for Visual Detection of Cobalt(II) Ions and PH Sensing. *Microchem. J.* **2019**, *147*, 183−190.

(21) Liu, Z.; Zhou, X.; Wu, F.; Liu, Z. Microwave-Assisted Preparation of Activated Carbon Modified by Zinc Chloride as a Packing Material for Column Separation of Saccharides. *ACS Omega* **2020**, *5* (17), 10106−10114.

(22) Thue, P. S.; Adebayo, M. A.; Lima, E. C.; Sieliechi, J. M.; Machado, F. M.; Dotto, G. L.; Vaghetti, J. C. P.; Dias, S. L. P. Preparation, Characterization and Application of Microwave-Assisted Activated Carbons from Wood Chips for Removal of Phenol from Aqueous Solution. *J. Mol. Liq.* **2016**, *223*, 1067−1080.

(23) Zhu, Z.; Niu, H.; Li, R.; Yang, Z.; Wang, J.; Li, X.; Pan, P.; Liu, J.; Zhou, B. One-Pot Hydrothermal Synthesis of Fluorescent Carbon Quantum Dots with Tunable Emission Color for Application in Electroluminescence Detection of Dopamine. *Biosens. Bioelectron.: X* **2022**, *10* (January), No. 100141, DOI: 10.1016/j.biosx.2022.100141.

(24) Mishra, V. K.; Rai, S. B.; Asthana, B. P.; Parkash, O.; Kumar, D. Effect of Annealing on Nanoparticles of Hydroxyapatite Synthesized via Microwave Irradiation: Structural and Spectroscopic Studies. *Ceram. Int.* **2014**, *40* (7 PART B), 11319−11328.

(25) Wang, H. J.; Hou, W. Y.; Yu, T. T.; Chen, H. L.; Zhang, Q. Q. Facile Microwave Synthesis of Carbon Dots Powder with Enhanced Solid-State Fluorescence and Its Applications in Rapid Fingerprints Detection and White-Light-Emitting Diodes. *Dyes Pigm.* **2019**, *170*, No. 107623, DOI: 10.1016/j.dyepig.2019.107623.

(26) Khan, M. E.; Mohammad, A.; Yoon, T. State-of-the-Art Developments in Carbon Quantum Dots (CQDs): Photo-Catalysis, Bio-Imaging, and Bio-Sensing Applications. *Chemosphere* **2022**, *302* (May), No. 134815.

(27) Li, L.; Zhang, R.; Lu, C.; Sun, J.; Wang, L.; Qu, B.; Li, T.; Liu, Y.; Li, S. In Situ Synthesis of NIR-Light Emitting Carbon Dots Derived from Spinach for Bio-Imaging Applications. *J. Mater. Chem. B* **2017**, *5* (35), 7328−7334.

(28) Zhang, Q.; Tian, F.; Zhou, Q.; Zhang, C.; Tang, S.; Jiang, L.; Du, S. Targeted Ginkgo Kernel Biomass Precursor Using Eco-Friendly Synthesis of Efficient Carbon Quantum Dots for Detection of Trace Nitrite Ions and Cell Imaging. *Inorg. Chem. Commun.* **2022**, *140* (December 2021), No. 109442.

(29) Kailasa, S. K.; Koduru, J. R. Perspectives of Magnetic Nature Carbon Dots in Analytical Chemistry: From Separation to Detection and Bioimaging. *Trends Environ. Anal. Chem.* **2022**, *33*, No. e00153.

(30) Bao, L.; Liu, C.; Zhang, Z. L.; Pang, D. W. Photoluminescence-Tunable Carbon Nanodots: Surface-State Energy-Gap Tuning. *Adv. Mater.* **2015**, *27* (10), 1663−1667.

(31) Hassan, M.; Gomes, V. G.; Dehghani, A.; Ardekani, S. M. Engineering Carbon Quantum Dots for Photomediated Theranostics. *Nano Res.* **2018**, *11* (1), 1−41, DOI: 10.1007/s12274-017-1616-1.

(32) Zulfajri, M.; Sudewi, S.; Ismulyati, S.; Rasool, A.; Adlim, M.; Huang, G. G. Carbon Dot/Polymer Composites with Various

https://doi.org/10.1021/acsomega.4c02254
ACS Omega 2024, 9, 20571−20581

Precursors and Their Sensing Applications: A Review. *Coatings* **2021**, *11* (9), No. 1100, DOI: 10.3390/coatings11091100.
(33) Atchudan, R.; Edison, T. N. J. I.; Chakradhar, D.; Perumal, S.; Shim, J. J.; Lee, Y. R. Facile Green Synthesis of Nitrogen-Doped Carbon Dots Using Chionanthus Retusus Fruit Extract and Investigation of Their Suitability for Metal Ion Sensing and Biological Applications. *Sens. Actuators, B* **2017**, *246*, 497−509.
(34) Murugan, N.; Prakash, M.; Jayakumar, M.; Sundaramurthy, A.; Sundramoorthy, A. K. Green Synthesis of Fluorescent Carbon Quantum Dots from Eleusine Coracana and Their Application as a Fluorescence 'Turn-off' Sensor Probe for Selective Detection of Cu 2+. *Appl. Surf. Sci.* **2019**, *476* (September 2018), 468−480.
(35) Yusuf, V. F.; Atulbhai, S. V.; Swapna, B.; Malek, N. I.; Kailasa, S. K. Recent Developments in Carbon Dot-Based Green Analytical Methods: New Opportunities in Fluorescence Assays of Pesticides, Drugs and Biomolecules. *New J. Chem.* **2022**, *46* (30), 14287−14308.
(36) Sun, C.; Gao, X.; Wang, L.; Zhou, N. Rapid Response and High Selectivity for Reactive Nitrogen Species Based on Carbon Quantum Dots Fluorescent Probes. *Food Anal. Methods* **2021**, *14* (6), 1121−1132.
(37) Iqbal, A.; Tian, Y.; Wang, X.; Gong, D.; Guo, Y.; Iqbal, K.; Wang, Z.; Liu, W.; Qin, W. Carbon Dots Prepared by Solid State Method via Citric Acid and 1,10-Phenanthroline for Selective and Sensing Detection of Fe2+ and Fe3+. *Sens. Actuators, B* **2016**, *237*, 408−415.
(38) Qi, H.; Teng, M.; Liu, M.; Liu, S.; Li, J.; Yu, H.; Teng, C.; Huang, Z.; Liu, H.; Shao, Q.; Umar, A.; Ding, T.; Gao, Q.; Guo, Z. Biomass-Derived Nitrogen-Doped Carbon Quantum Dots: Highly Selective Fluorescent Probe for Detecting Fe 3+ Ions and Tetracyclines. *J. Colloid Interface Sci.* **2019**, *539*, 332−341.
(39) Bandi, R.; Gangapuram, B. R.; Dadigala, R.; Eslavath, R.; Singh, S. S.; Guttena, V. Facile and Green Synthesis of Fluorescent Carbon Dots from Onion Waste and Their Potential Applications as Sensor and Multicolour Imaging Agents. *RSC Adv.* **2016**, *6* (34), 28633−28639.
(40) Ravi, S.; Jayaraj, M. K. Sustainable Carbon Dots as "Turn-off" Fluorescence Sensor for Highly Sensitive Pb2+ Detection. *Emergent Mater.* **2020**, *3* (1), 51−56.
(41) Tyagi, A.; Tripathi, K. M.; Singh, N.; Choudhary, S.; Gupta, R. K. Green Synthesis of Carbon Quantum Dots from Lemon Peel Waste: Applications in Sensing and Photocatalysis. *RSC Adv.* **2016**, *6* (76), 72423−72432.
(42) Wang, S.; Niu, H.; He, S.; Cai, Y. One-Step Fabrication of High Quantum Yield Sulfur- and Nitrogen-Doped Carbon Dots for Sensitive and Selective Detection of Cr(VI). *RSC Adv.* **2016**, *6* (109), 107717−107722.
(43) Nazar, M.; Nada, C. E.; Syahrial, Rusman.; Khaldun, I.; Hasan, M.; Wirjosentono, B.; Basri. Carbon Quantum Dots Synthesis Optimization Using Response Surface Methodology. *AIP Conf. Proc.* **2024**, *3082* (1), No. 040016, DOI: 10.1063/5.0201545.
(44) Nazar, M.; Aulya, N. M.; Syahrial; Puspita, K. REMOVAL OF METHANAL FROM AQUEOUS SOLUTION USING MICRO-WAVE INDUCED CARBON FROM Coffea Arabica GROUNDS WASTE. *Rasayan Journal of Chemistry* **2022**, *15* (1), 221−231.
(45) Rhys Williams, A. T.; Winfield, S. A.; Miller, J. N. Relative Fluorescence Quantum Yields Using a Computer-Controlled Luminescence Spectrometer. *Analyst* **1983**, *108* (1290), 1067−1071.
(46) Melhuish, W. H. Quantum Efficiencies of Fluorescence of Organic Substances: Effect of Solvent and Concentration of The Fluorescent Solute. *J. Phys. Chem. A* **1961**, *65*, 229−235, DOI: 10.1021/j100820a009.
(47) Zulfajri, M.; Gedda, G.; Chang, C. J.; Chang, Y. P.; Huang, G. G. Cranberry Beans Derived Carbon Dots as a Potential Fluorescence Sensor for Selective Detection of Fe3+ Ions in Aqueous Solution. *ACS Omega* **2019**, *4* (13), 15382−15392.
(48) VA, A.; P, S.; Poovathinthodiyil, R.; N K, R. Table Sugar Derived Carbon Dot—A Promising Green Reducing Agent. *Mater. Res. Bull.* **2021**, *139*, No. 111284, DOI: 10.1016/j.materres-bull.2021.111284.
(49) Jusuf, B. N.; Sambudi, N. S.; Isnaeni, I.; Samsuri, S. Microwave-Assisted Synthesis of Carbon Dots from Eggshell Membrane Ashes by Using Sodium Hydroxide and Their Usage for Degradation of Methylene Blue. *J. Environ. Chem. Eng.* **2018**, *6* (6), 7426−7433.
(50) Nammahachak, N.; Aup-Ngoen, K. K.; Asanithi, P.; Horpratum, M.; Chuangchote, S.; Ratanaphan, S.; Surareungchai, W. Hydrothermal Synthesis of Carbon Quantum Dots with Size Tunability via Heterogeneous Nucleation. *RSC Adv.* **2022**, *12* (49), 31729−31733.
(51) Chunduri, L. A. A.; Kurdekar, A.; Patnaik, S.; Aditha, S.; Prathibha, C.; Kamisetti, V. Keywords Single Step Synthesis of Carbon Quantum Dots from Coconut Shell: Evaluation for Antioxidant Efficacy and Hemotoxicity Citation-. *J. Mater. Sci. Appl.* **2017**, *3* (6), 83−93.
(52) Arumugam, N.; Kim, J. Synthesis of Carbon Quantum Dots from Broccoli and Their Ability to Detect Silver Ions. *Mater. Lett.* **2018**, *219*, 37−40.
(53) Raikwar, V. R. Synthesis and Study of Carbon Quantum Dots (CQDs) for Enhancement of Luminescence Intensity of CQD@ LaPO4:Eu3+ Nanocomposite. *Mater. Chem. Phys.* **2022**, *275*, No. 125277.
(54) Kaushik, A.; Basu, S.; Singh, K.; Batra, V. S.; Balakrishnan, M. Activated Carbon from Sugarcane Bagasse Ash for Melanoidins Recovery. *J. Environ. Manage.* **2017**, *200*, 29−34.
(55) Xu, H.; Xie, L.; Hakkarainen, M. Coffee-Ground-Derived Quantum Dots for Aqueous Processable Nanoporous Graphene Membranes. *ACS Sustainable Chem. Eng.* **2017**, *5* (6), 5360−5367, DOI: 10.1021/acssuschemeng.7b00663.
(56) Singh, K. J.; Ahmed, T.; Gautam, P.; Sadhu, A. S.; Lien, D. H.; Chen, S. C.; Chueh, Y. L.; Kuo, H. C. Recent Advances in Two-dimensional Quantum Dots and Their Applications. *Nanomaterials* **2021**, *11* (6), No. 1549, DOI: 10.3390/nano11061549.
(57) Sutanto, H.; Alkian, I.; Romanda, N.; Lewa, I. W. L.; Marhaendrajaya, I.; Triadyaksa, P. High Green-Emission Carbon Dots and Its Optical Properties: Microwave Power Effect. *AIP Adv.* **2020**, *10* (5), No. 055008, DOI: 10.1063/5.0004595.
(58) Kim, T. H.; Wang, F.; McCormick, P.; Wang, L.; Brown, C.; Li, Q. Salt-Embedded Carbon Nanodots as a UV and Thermal Stable Fluorophore for Light-Emitting Diodes. *J. Lumin.* **2014**, *154*, 1−7.
(59) Rimal, V.; Shishodia, S.; Srivastava, P. K. Novel Synthesis of High-Thermal Stability Carbon Dots and Nanocomposites from Oleic Acid as an Organic Substrate. *Appl. Nanosci.* **2020**, *10* (2), 455−464.
(60) Khan, W. U.; Wang, D.; Wang, Y. Highly Green Emissive Nitrogen-Doped Carbon Dots with Excellent Thermal Stability for Bioimaging and Solid-State LED. *Inorg. Chem.* **2018**, *57* (24), 15229−15239.
(61) Perikala, M.; Bhardwaj, A. Highly Stable White-Light-Emitting Carbon Dot Synthesis Using a Non-Coordinating Solvent. *ACS Omega* **2019**, *4* (25), 21223−21229.
(62) Dua, S.; Kumar, P.; Pani, B.; Kaur, A.; Khanna, M.; Bhatt, G. Stability of Carbon Quantum Dots: A Critical Review. *RSC Adv.* **2023**, *13*, 13845−13861, DOI: 10.1039/D2RA07180K.
(63) Chukwuocha, E. O.; Onyeaju, M. C.; Harry, T. S. T. Theoretical Studies on the Effect of Confinement on Quantum Dots Using the Brus Equation. *World J. Condens. Matter Phys.* **2012**, *02* (02), 96−100.
(64) Terna, A. D.; Elemike, E. E.; Mbonu, J. I.; Osafile, O. E.; Ezeani, R. O. The Future of Semiconductors Nanoparticles: Synthesis, Properties and Applications. *Mater. Sci. Eng.: B* **2021**, *272*, No. 115363.
(65) Pang, Y. X.; Li, X.; Zhang, X.; Yeoh, J. X.; Wong, C.; Manickam, S.; Yan, Y.; Wu, T.; Pang, C. H. The Synthesis of Carbon-Based Quantum Dots: A Supercritical Fluid Approach and Perspective. *Mater. Today Phys.* **2022**, *27* (June), No. 100752, DOI: 10.1016/j.mtphys.2022.100752.
(66) Abd Rani, U.; Ng, L. Y.; Ng, Y. S.; Ng, C. Y.; Ong, Y. H.; Lim, Y. P. Photocatalytic Degradation of Methyl Green Dye by Nitrogen-Doped Carbon Quantum Dots: Optimisation Study by Taguchi Approach. *Mater. Sci. Eng. B* **2022**, *283* (June), No. 115820.

(67) Gaur, N. S.; Chhipa, R. C. *Synthesis and Significance of Carbon Quantum Dots (A Review) Synthesis and Significance of Carbon Quantum Dots (A Review)* 2020.
(68) Arcudi, F.; Dordevic, L.; Prato, M. Synthesis, Separation, and Characterization of Small and Highly Fluorescent Nitrogen-Doped Carbon Nanodots. *Angew. Chem., Int. Ed.* **2016**, *55* (6), 2107−2112.
(69) Hoan, B. T.; Tam, P. D.; Pham, V. H. Green Synthesis of Highly Luminescent Carbon Quantum Dots from Lemon Juice. *J. Nanotechnol.* **2019**, *2019*, No. 2852816, DOI: 10.1155/2019/2852816.
(70) Hsu, P. C.; Shih, Z. Y.; Lee, C. H.; Chang, H. T. Synthesis and Analytical Applications of Photoluminescent Carbon Nanodots. *Green Chem.* **2012**, *14* (4), 917−920.
(71) Costa, A. I.; Barata, P. D.; Moraes, B.; Prata, J. V. Carbon Dots from Coffee Grounds: Synthesis, Characterization and Detection of Noxious Nitroanilines. *Chemosensors* **2022**, *10* (3), No. 113, DOI: 10.3390/chemosensors10030113.
(72) Sachdev, A.; Gopinath, P. Green Synthesis of Multifunctional Carbon Dots from Coriander Leaves and Their Potential Application as Antioxidants, Sensors and Bioimaging Agents. *Analyst* **2015**, *140* (12), 4260−4269.
(73) Vadia, F. Y.; Ghosh, S.; Mehta, V. N.; Jha, S.; Malek, N. I.; Park, T. J.; Kailasa, S. K. Fluorescence "Turn OFF-ON" Detection of Fe3+ and Propiconazole Pesticide Using Blue Emissive Carbon Dots from Lemon Peel. *Food Chem.* **2023**, *428*, No. 136796.
(74) Khan, Z. M. S. H.; Rahman, R. S.; Shumaila; Islam, S.; Zulfequar, M. Hydrothermal Treatment of Red Lentils for the Synthesis of Fluorescent Carbon Quantum Dots and Its Application for Sensing Fe3+. *Opt. Mater.* **2019**, *91*, 386−395.
(75) Wang, Q.; Wang, Z.; Pu, Z.; Wang, Y.; Li, M. Lanthanum-Doped Carbon Quantum Dots (La-CQDs) for Detection of Fe3+ in Colorimetric Test Paper and Information Anti-Counterfeiting. *Opt. Mater.* **2023**, *137*, No. 113630.

https://doi.org/10.1021/acsomega.4c02254
ACS Omega 2024, 9, 20571−20581